Early stages of precipitation in Mg-RE alloys studied by positron annihilation spectroscopy

M Vlček[1], J Čížek[1], O Melikhova[1], P Hruška[1], I Procházka[1], M Vlach[1], I Stulíková[1], B Smola[1]
[1]Charles University in Prague, Faculty of Mathematics and Physics, V Holešovičkách 2, 18000 Praha 8, Czech Republic

E-mail: marian.vlcek@gmail.com

Abstract. Magnesium alloys with rare earth (RE) elements are promising structural materials exhibiting favourable mechanical properties at elevated temperatures. However, the processes occurring during early stages of precipitation in these alloys are still not completely understood. In this work positron lifetime spectroscopy combined with coincidence Doppler broadening was employed for investigation of early stages of precipitation in Mg-RE alloys. Presence of quenched-in vacancy clusters was observed after solution treatment of studied alloys. These quenched-in vacancy clusters are bound to RE solutes and thereby stabilized at room temperature. During natural aging, RE clusters are formed by vacancy-assisted long-range diffusion. In addition, hardness of studied materials increases and quenched-in vacancy clusters are annealed out during the course of natural aging. Simple model was developed to describe hardening during natural aging.

1. Introduction

Mg-based alloys with rare earth (RE) alloying elements, e.g. Gd and Tb, represent promising light hardenable alloys with a high creep resistance at elevated temperatures [1]. Since the solubility limit of RE alloying elements in Mg strongly decreases at low temperatures, supersaturated solid solution of RE solutes in α-Mg matrix can be formed by fast quenching from elevated temperatures. During subsequent heating the supersaturated solid solution decomposes by formation of a sequence of metastable phases which may cause significant hardening of the alloy. For example the supersaturated solid solution of Gd in Mg decomposes in the sequence [2]:

$$\alpha'(\mathrm{hcp}) \rightarrow \beta''(\mathrm{DO}_{19}\ \mathrm{clusters}) \rightarrow \beta'(\mathrm{c\text{-}bco}) \rightarrow \beta\ (\mathrm{fcc}, \mathrm{Mg_5Gd\ type}). \qquad (1)$$

The β'' particles are coherent with the α-Mg matrix while for the β' and β precipitates the coherency with the α-Mg matrix is partially lost. Although the precipitation sequences are nowadays well documented for various Mg-RE systems, there is still a lack of information about very early stages of decomposition leading eventually to formation of coherent metastable particles usually with DO_{19} structure.

Natural aging is a process where solute atoms and vacancies cluster at room temperature in materials quenched from high annealing temperature. It is well known effect and was thoroughly investigated in Al-based alloys [3, 4, 5, 6]. Significant strengthening occurs because solute clusters developed during natural aging hinder movement of dislocations. Contrary to Al-based alloys, natural

aging of Mg-based alloys is not common. So far, natural aging was observed in Mg-Zn-based alloys [7] and, recently, in our work in Mg-Gd and Mg-Tb alloys [8]. In this work positron lifetime spectroscopy combined with coincidence Doppler broadening was employed for investigation of early stages of precipitation in Mg-RE alloys.

2. Experimental details

Binary Mg-Gd and Mg-Tb were produced by squeeze casting under a protective atmosphere (Ar + 1% SF_6). Chemical composition of studied alloys is shown in table 1.

Table 1. Composition of studied alloys.

	Gd		Tb		Mg
	wt.%	**at.%**	**wt.%**	**at.%**	
Mg4Gd	4.48	0.72	-	-	balance
Mg9Gd	9.24	1.55	-	-	balance
Mg15Gd	14.58	2.57	-	-	balance
Mg13Tb	-	-	13.39	2.31	balance

The as-cast Mg-Gd and Mg-Tb alloys were subjected to solution treatment at 500 and 530°C, respectively, for 6 hours finished by quenching into water at room temperature. Samples were subsequently naturally aged at ambient temperature.

Positron lifetime spectroscopy measurements were performed using a digital positron lifetime spectrometer [9] with excellent time resolution of 145 ps (FWHM of the resolution function obtained from fitting of positron lifetime spectrum of a well-annealed Mg reference sample). At least 10^7 annihilation events were accumulated in each spectrum. Source
contribution consisting of two components with lifetimes 368 ps and 1.5 ns with relative intensities 8% and 1%, respectively, which originated from positrons annihilated in the $^{22}Na_2CO_3$ positron source deposited on a 2 μm thick mylar foil, was substracted from the spectra.

Coincidence Doppler broadening (CDB) measurements were carried out using a digital spectrometer [10] equipped with two HPGe detectors with the resolution of 0.9 keV at 511 keV (FWHM). The total statistics accumulated in each two-dimensional CDB spectrum was at least 10^8 positron annihilation events in each spectrum.

The Vickers microhardness (HV) testing was carried out using a STRUERS Duramin 300 hardness tester with a load of 100 g applied for 10 s.

3. Results

Time development of hardness of solution treated samples aged at ambient temperature is shown in figure 1a. Hardness of all studied alloys clearly increases with increasing aging time. The time dependence of microhardness plotted in the logarithmic time scale exhibits characteristic S-shaped curve typical for natural aging.

The hardness of alloy aged for time t can be expressed as:

$$HV(t) = HV_0 + \Delta HV(t), \tag{2}$$

where $HV_0 = 30 \pm 2$ is the hardness of pure Mg matrix and $\Delta HV(t)$ denotes hardening caused by solute elements:

$$\Delta HV(t) = (HV_{ss}^2 + HV_{cl}^2)^{1/2}. \tag{3}$$

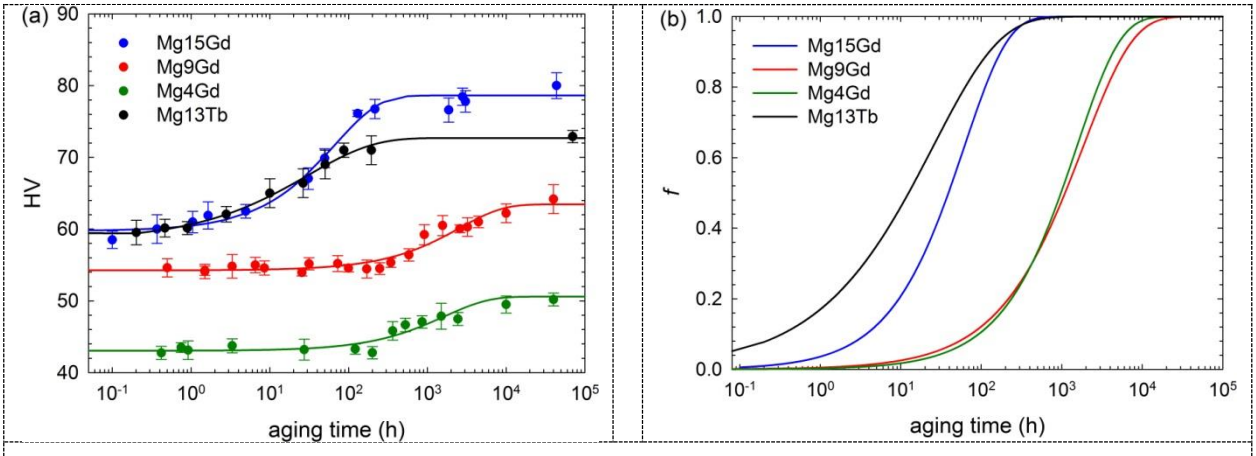

Figure 1. (a) Comparison of microhardness evolution during natural aging of studied alloys. (b) Time development of relative volume fraction of clusters obtained from fitting.

The symbols HV_{ss} and HV_{cl} denote contribution to the hardening caused by solid solution hardening and by clusters of alloying elements, respectively. Let f denote the relative fraction of solute atoms present in clusters. The hardening caused by clusters HV_{cl} is then proportional to $f^{1/2}$ while the solid solution hardening HV_{ss} is proportional to $(1-f)^{2/3}$ [3]. Hence, the evolution of the hardness during aging can be written as:

$$HV(t) = HV_0 + \left[\left(h_{ss}c^{2/3}(1-f)^{2/3}\right)^2 + \left(h_{cl}\left(\frac{c}{N_{cl}}\right)^{1/2} f^{1/2}\right)^2\right]^{1/2}, \quad (4)$$

where c is the total concentration of alloying element (Gd or Tb) in at.%, h_{ss} and h_{cl} are hardening coefficients for solid solution hardening and hardening by clusters, respectively, and N_{cl} is the average number of atoms per cluster.

Table 2. Fitted parameters of hardening model.

	h_{ss}	$h_{cl}/(N_{cl})^{1/2}$	k (s^{-1})	n
Mg4Gd	350(10)	243(8)	$1.8(7)\times10^{-7}$	0.8(3)
Mg9Gd	390(5)	269(5)	$1.5(4)\times10^{-7}$	0.7(1)
Mg15Gd	342(8)	301(3)	$4.5(7)\times10^{-6}$	0.8(1)
Mg13Tb	360(10)	286(4)	$1.1(2)\times10^{-5}$	0.52(8)

The clusters in aged alloys develop by nucleation and subsequent growth. Since the studied alloys are coarse grained and exhibit low dislocation density, it is reasonable to assume that heterogeneous nucleation in limited number of suitable nucleation sites takes place. These sites are used at the early stage of clustering and so called site saturation occurs. Under these assumptions, the relative volume fraction of clusters is given by expression:

$$f = 1 - \exp[-(k(T)t)^n], \quad (5)$$

where $k(T)$ is the kinetic rate at temperature T and n is the kinetic exponent [3]. The quantity f is also identical to the relative fraction of solute atoms which precipitated from the solid solution and formed

clusters. Hence, when $f = 0$ all solute atoms are in solid solution and no clusters are present in the sample, while the clusters are fully developed and no solutes remain in solid solution when $f = 1$.

Results obtained by fitting the measured data with proposed model of hardening are shown in table 2. The relative volume fraction of clusters f obtained from fitting is shown in figure 1b. As an example, fits of data measured on Mg15Gd and Mg13Tb alloys showing individual contributions HV_0, HV_{ss} and HV_{cl} to the total hardness are shown in figures 2a and 2b, respectively.

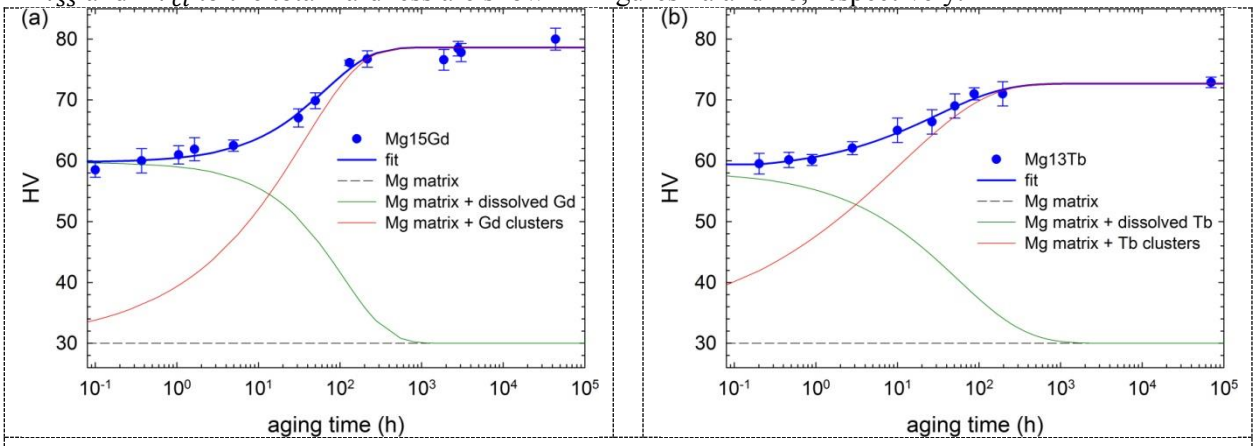

Figure 2. Development of microhardness and fit by the theoretical model described in the text: (a) Mg15Gd, (b) Mg13Tb.

Results obtained by positron lifetime spectroscopy are summarized in table 3. All quenched alloys exhibit two component positron lifetime spectra. The first component comes from free positrons while the second component represents a contribution of positrons trapped at defects. The lifetime of the second component $\tau_2 \approx 300$ ps agrees well with the theoretically calculated lifetime for a monovacancy in Mg [11]. However, experimental results suggest that positron lifetime for a monovacancy in Mg is ≈ 255 ps [12]. Therefore, positron lifetime measurements testify to presence of quenched-in vacancies or small vacancy clusters in the quenched alloys.

On the other hand, the alloys aged at ambient temperature for 2 months exhibit single component spectra with lifetime $\tau_1 \approx 225$ ps which agrees well with the bulk positron lifetime in Mg [11]. Hence, they are defect free within the sensitivity of positron lifetime spectroscopy.

Table 3. Results of positron lifetime measurements.

	quenched alloys				aged alloys (2 months)	
	τ_1 (ps)	I_1 (%)	τ_2 (ps)	I_2 (%)	τ_1 (ps)	I_1 (%)
Mg4Gd	219.7(5)	92.5(5)	290(10)	7.5(5)	225.5(2)	100
Mg9Gd	218.6(5)	88.4(5)	300(5)	11.6(5)	225.2(2)	100
Mg15Gd	214.6(7)	80.5(6)	295(5)	19.5(6)	225.4(2)	100
Mg13Tb	214.0(8)	84.3(7)	280(15)	15.7(7)	225.5(2)	100

Results of coincidence Doppler broadening measurements performed on Mg15Gd and Mg13Tb alloys are shown in figures 3a and 3 b, respectively. Ratio curves of quenched alloys show peak located at $p \approx 8 \times 10^{-3}\ m_0 c$ which testifies to enhanced concentration of Gd or Tb around quenched-in vacancy clusters. Amplitude of this peak significantly decreases after aging due to disappearance of quenched-in vacancy clusters.

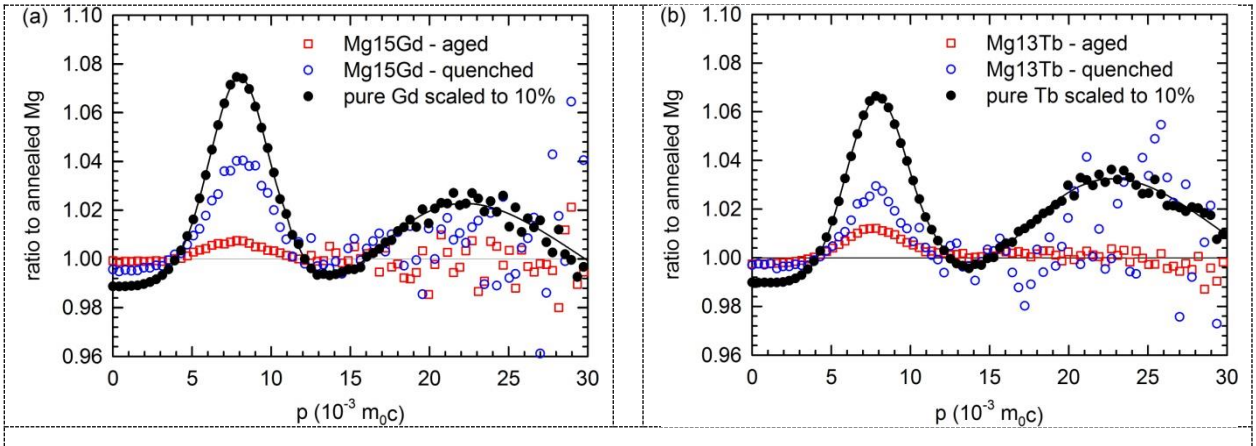

Figure 3. Coincidence Doppler broadening ratio curves: (a) Mg15Gd, (b) Mg13Tb.

Under the assumption that vacancy-Gd (or Tb) complexes consist of Mg monovacancy and a solute atom, concentration of quenched-in vacancy-Gd (or Tb) complexes can be calculated from positron lifetime data according to the simple trapping model [13]:

$$c_{pairs} = \frac{1}{\nu_v} I_2 \left(\frac{1}{\tau_1} - \frac{1}{\tau_2}\right), \tag{6}$$

where $\nu_v = 1.1 \times 10^{13}$ s^{-1} is the specific positron trapping rate for vacancy in Mg [14].

Note that the specific positron trapping rate for a small cluster composed of N vacancies is $N\nu_v$. Therefore, trapping rate to vacancies of fixed concentration is the same independently whether they exist as isolated monovacancies or form small vacancy clusters providing that positron trapping is in transition limited regime [15], i.e. the mutual distance among vacancy clusters is significantly smaller than the mean positron diffusion length.

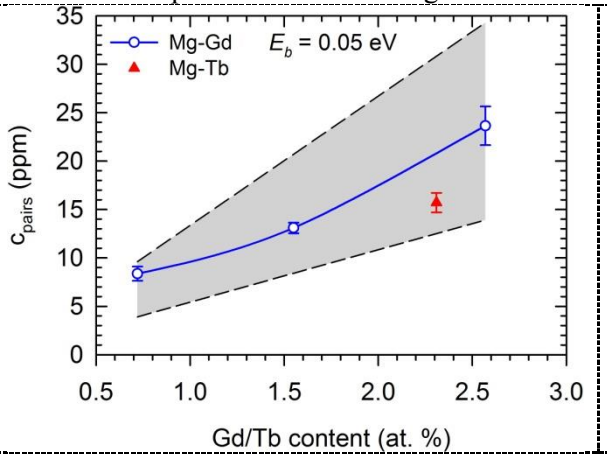

Figure 4. The concentration quenched-in vacancy-Gd (open circles) and vacancy-Tb (full triangle) pairs measured by positron lifetime spectroscopy. Shaded region shows the band for equilibrium concentration of vacancy-solute pairs at 500°C calculated by equation (7). Binding energy E_b between vacancy and Gd or Tb was assumed to be 0.05 eV.

Values calculated according to equation 6 can be compared to the equilibrium concentration of vacancy-Gd (or Tb) pairs at solution treatment temperature T given by expression:

$$c^*_{pairs} = c \exp\left(\frac{S_{v,f}}{k_B}\right) \exp\left(-\frac{E_{v,f} - E_b}{k_B T}\right), \tag{7}$$

where k_B is the Boltzmann constant, $S_{v,f} \approx 2k_B$ is the vacancy formation entropy [16]. The values of vacancy formation enthalpy $E_{v,f}$ reported in literature fall into the range 0.79-0.85 eV [12,17,18]. E_b is

the binding energy between vacancy and Gd or Tb. The latter quantity is not known, but putting $E_b = 0.05\,\mathrm{eV}$, i.e. assuming small attractive interaction between vacancy and Gd or Tb atom, the equilibrium concentration of vacancy-Gd(Tb) pairs given by equation (7) falls into the shaded area in figure 4 which is in good agreement with experimental data.

4. Discussion

All studied Mg-RE alloys exhibit natural aging and the magnitude of hardening during aging as well as the concentration of quenched-in vacancy clusters increase with increasing concentration of RE alloying elements. It was found that early stages of precipitation are controlled by quenched-in vacancies. Positive binding energy between vacancy and solute atoms facilitates creation of solute-vacancy complexes during solution treatment at elevated temperature. However, since the binding energy between vacancy and Gd or Tb is comparable to the thermal energy most vacancies are not bound to Gd or Tb solutes during the solution treatment. In quenched samples free vacancies are quickly annealed out at room temperature but they can also bind to RE solutes. Vacancies associated with RE solutes are more stable and facilitate diffusivity of the solute RE atoms. Hence, the early stages of precipitation are strongly affected by the concentration of quenched-in vacancies bound to RE solutes. Agglomeration of solutes to small clusters proceeds by vacancy-assisted long-range diffusion. Solute clusters with defected structure containing vacancies are formed in the initial stage and further develop into precursors of the coherent DO_{19} precipitates.

Ab-initio theoretical calculations of positron lifetime for vacancy clusters with different sizes were performed to estimate the number of vacancies in vacancy-Gd (or Tb) complexes. Positron lifetimes were calculated within the so-called standard scheme [19] employing the atomic superposition method [20]. The electron-positron correlation was treated using the local density approximation according to the parametrization by Boroński and Nieminen [21]. The calculations were performed in 512 Mg atom based supercells. Vacancies and vacancy clusters were modeled simply by removing the corresponding number of atoms from the supercell.

Results of these calculations are presented in figure 5. Measured positron lifetime of defect component in quenched samples agrees well with the lifetime of $\approx 300\,\mathrm{ps}$ calculated for a Mg monovacancy. Note that similar lifetime was calculated for Mg monovacancy in reference [11].

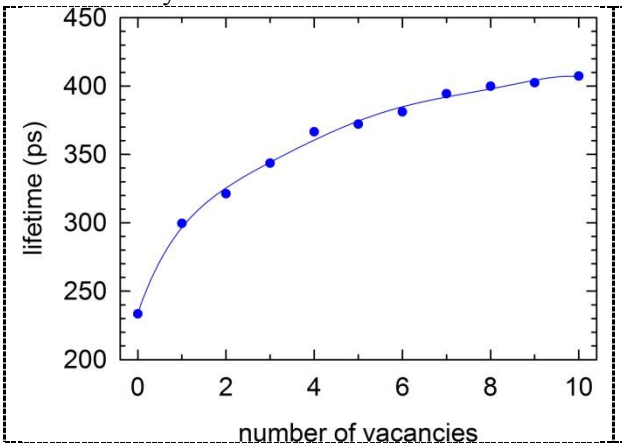

Figure 5. Calculated dependence of positron lifetime on the number of Mg vacancies in vacancy cluster. The solid line is just to guide the eyes.

On the other hand, the experimental lifetime value of $\approx 255\,\mathrm{ps}$ was determined by in-situ positron lifetime study of Mg samples annealed in the temperature range 0-600°C through fitting of the temperature dependence of the mean positron lifetime [12]. Low temperature measurements of quenched and electron irradiated Mg samples performed in reference [12] revealed defect component with positron lifetime of $(350 \pm 20)\,\mathrm{ps}$. Comparison with theoretical calculations suggests that in quenched and irradiated samples positron trapping occurs at complex small vacancy clusters consisting of 2-3 vacancies.

Nevertheless, the large difference between experimental and theoretical lifetimes for Mg monovacancy is very remarkable. In addition, the experimental value ≈ 255 ps determined in reference [12] is practically the same as the positron lifetime determined experimentally for dislocations in Mg which is ≈ 250 ps [22, 23, 24]. Therefore, further investigations are needed to definitively resolve these discrepancies and firmly assign the positron lifetime for vacancy in Mg. Hence, at the present stage of knowledge we can conclude that quenched Mg-Gd and Mg-Tb alloys studied here contain either monovacancies or small vacancy clusters (consisting of 2-3 vacancies) bound to Gd or Tb solutes.

The kinetics of natural aging is not the same for all studied alloys. The Mg15Gd and Mg13Tb alloys show significantly shorter incubation period of hardening than Mg4Gd and Mg9Gd alloys. This is most likely caused by higher concentration of alloying elements and thereby also higher concentration of quenched-in vacancies bound to RE solutes. However, further studies are required to elucidate the factors influencing the kinetics of natural aging in Mg-RE alloys.

5. Conclusions

Natural aging of Mg-Gd and Mg-Tb alloys associated with clustering of solute atoms was observed in this work. Theoretical model of hardening during natural aging showing good agreement with experimental data was developed.

Presence of quenched-in vacancy/vacancy cluster-Gd (or Tb) complexes in solution treated alloys was confirmed by positron annihilation spectroscopy. Quenched-in vacancies or vacancy clusters composed of up to three vacancies facilitate diffusion of Gd or Tb atoms in Mg matrix and disappear when the development of solute clusters is finished.

6. Acknowledgements

The research leading to these results has received funding from the People Programme (Marie Curie Actions) of the European Union's Seventh Framework Programme FP7/2007-2013/ under REA grant agreement N° 289163.

One of the authors (P. Hruška) acknowledges support by the Grant Agency of the Charles University (project no. 324015).

7. References

[1] Mordike B 2002 *Mat. Sci. Eng. A* **324** 103
[2] Vostrý P, Stulíková I, Smola B, von Buch F and Mordike B L 1999 *Phys. Status Solidi A* **175** 491
[3] Esmaeili S, Lloyd D J and Poole W J 2003 *Acta Materialia* **51** 3467
[4] Stulíková I, Faltus J and Smola B 2003 *Kovove Mater.* **45** 85
[5] Klobes B, Staab T E M, Haaks M, Maier K and Wieler I 2008 *Phys. Status Solidi RRL* **2** 224
[6] Banhart J, Lay M D H, Chang C S T and Hill J *2011 Phys. Rev. B* **83** 014101
[7] Buha J 2008 *J. Mater. Sci.* **43** 1120
[8] Čížek J, Smola B, Stulíková I, Hruška P, Vlach M, Vlček M, Melikhova O and Procházka I 2012 *Phys. Status Solidi A* **209** 2135
[9] Bečvář F, Čížek J, Procházka I and Janotová J 2005 *Nucl. Instr. Meth. Phys. Res. A* **539** 372
[10] Čížek J, Vlček M and Procházka I 2010 *Nucl. Instrum. Methods A* **623** 982
[11] Robles J M C, Ogando E and Plazaola F 2007 *J. Phys.: Condens. Matter* **19** 176222
[12] Hautojärvi P, Johansson J, Vehanen A and Yli-Kauppila J 1982 *Appl. Phys. A* **27** 49
[13] West R 1979 Positrons in Solids ed Hautojärvi P (Berlin: Springer-Verlag) p 89
[14] Hood G M 1982 *Phys. Rev. B* **26** 1036
[15] Dupasquier A, Romero R and Somoza A 1993 *Phys. Rev. B* **48** 9235
[16] Wollenberger H 1983 *Physical Metalurgy* vol 2 (Amsterdam: North-Holland) p 1146
[17] Tzanetakis P, Hillairet J and Revel G 1976 *Phys. Status Solidi B* **75** 433
[18] Tzanetakis P 1978 *Thése* (Université de Grenoble)

[19] Puska M J and Nieminen R M 1994 *Rev. Mod. Phys.* **66** 841
[20] Puska M J and Nieminen R M 1983 J. *Phys. F: Met. Phys.* **13** 333
[21] Boroński E and Nieminen R M 1986 *Phys. Rev. B* **34** 3820
[22] Čížek J, Procházka I, Smola B, Stulíková I, Kužel R, Matěj Z and Cherkaska V 2006 *Phys. Status Solidi A* **203** 466
[23] del Río J, Gómez C and Ruano M 2012 *Philos. Mag.* **92** 535
[24] Dryzek J and Dryzek E 2011 *Magnesium Alloys - Corrosion and Surface Treatments* (Rijeka: InTech) p 289